International Journal of Innovative Computing, Information and Control
Volume **13**, Number **3**, June **2017**

ICIC International ©2017 ISSN 1349-4198
pp. 1007–1019

DESIGN OF A HIGH-VOLTAGE MULTIPLIER COMBINED WITH COCKCROFT-WALTON VOLTAGE MULTIPLIERS AND SWITCHED-CAPACITOR AC-AC CONVERTERS

Kei Eguchi[1], Anan Wongjan[2], Amphawan Julsereewong[2]
Wanglok Do[1] and Ichirou Oota[3]

[1]Department of Information Electronics
Fukuoka Institute of Technology
3-30-1 Wajirohigashi, Higashi-ku, Fukuoka 811-0295, Japan
eguti@fit.ac.jp; dwl12345@naver.com

[2]Faculty of Engineering
King Mongkut's Institute of Technology Ladkrabang
Ladkrabang, Bangkok 1052, Thailand
anandata@hotmail.com; amphawan.ju@kmitl.ac.th

[3]Department of Information, Communication and Electronic Engineering
National Institute of Technology, Kumamoto College
2659-2 Suya, Koushi-shi, Kumamoto 861-1102, Japan
oota-i@kumamoto-nct.ac.jp

Received January 2017; revised April 2017

Abstract. *In recent years, the non-thermal food processing is receiving much attention, because the non-thermal food processing can offer nutritious and fresh processed foods at low cost. In the non-thermal food processing, an underwater shockwave is utilized by discharging a high voltage in water. To generate the underwater shockwave, this paper proposes a novel high voltage multiplier designed by connecting a bipolar Cockcroft-Walton voltage multiplier (CWVM) with a switched-capacitor (SC) direct ac-ac converter in series. In the proposed multiplier, first, an ac input is amplified to double by the inductor-less ac-ac converter. Then, the output of the ac-ac converter is stepped-up again by the bipolar CWVM. Therefore, owing to the inductor-less series-connected bipolar topology, the proposed multiplier can achieve smaller size and higher gain than existing multipliers. Concerning the proposed multiplier with* 26× *step-up gain, the operation principle and theoretical analysis are discussed in detail. Furthermore, the feasibility and effectiveness of the proposed multiplier are demonstrated by simulation program with integrated circuit emphasis (SPICE) simulations.*

Keywords: Series-connected bipolar topology, Cockcroft-Walton multipliers, Inductor-less ac-ac converter, Non-thermal food processing, Switched-capacitor circuits

1. **Introduction.** For the healthy life of people, effective food processing is a vital issue. In recent years, a food processing technology without heating [1] has been studied to offer nutritious and fresh foods to consumers. In the non-thermal food processing, the destruction of nutrients is not caused with an increase in temperature. Concerning the non-thermal food processing, there are many kinds of technologies [1], such as High Hydrostatic Pressure (HHP), High Voltage Arc Discharge (HVAD), and Cold Plasma (CP). Among others, non-thermal food processing utilizing an underwater shockwave is one of the most promising methods to provide nutritious and fresh foods at low cost. In the non-thermal food processing utilizing an underwater shockwave, the cell wall and organization of foods are destroyed by the high-speed destruction phenomenon that is called spalling

destruction [2-5]. To generate the underwater shockwave, a high voltage multiplier, such as the Cockcroft-Walton voltage multiplier (CWVM) [6], is used to cause the spalling destruction. The CWVM has light and simple circuit configuration, because a magnetic transformer with high turn ratio is not required to design CWVM.

In past studies, various types of CWVMs have been developed. For example, Wang and Luerkens proposed a cascade CWVM and its model of parasitic capacitances in 2013 [7] and Patel and Dave implemented a negative high voltage multiplier in 2013 [8]. Owing to the symmetrical structure, the cascade CWVM [7] can reduce the voltage ripple magnitude. Furthermore, the complete model of the parasitic capacitances was given in [7]. However, Wang and Luerkens's voltage multiplier requires a transformer with center-tapped secondary to perform its push-pull kind of operation. On the other hand, Patel and Dave's voltage multiplier can generate a negative stepped-up voltage [8]. However, a transformer with high turn ratio is necessary for the Patel and Dave's multiplier. Therefore, these voltage multipliers are heavy and bulky. Without using transformers, Young et al. suggested a boost type voltage multiplier based on the CWVM in 2009 [9] and 2011 [10]. By combining a boost converter and a CWVM, the voltage multipliers in [9,10] generate a high voltage with a small number of stages. Furthermore, unlike the conventional multipliers in [7,8], a transformer with high turn ratio is not necessary to design the boost type voltage multiplier based on the CWVM [9,10]. However, the voltage multipliers in [9,10] require a large inductor.

To reduce the voltage drop caused by the increase of the number of stages, Iqbal and Besar and Eguchi et al. suggested a bipolar CWVM in 2007 [11] and 2011 [12], because the output voltage of CWVM is lowered according to the increase of the number of stages. Unlike the above-mentioned voltage multipliers [6-10], the bipolar CWVM can offer a high stepped-up voltage by combining the outputs of positive and negative multipliers. Following this study, Iqbal developed a hybrid symmetrical CWVM in 2014 [13]. Owing to the hybrid symmetrical bipolar topology, Iqbal's high voltage multiplier can alleviate the voltage drop and can improve transient response from the conventional voltage multipliers [6-12]. However, due to the switching control using ac inputs, response speed is slow.

To improve the response speed, a high-speed voltage multiplier [14-16] is proposed by Eguchi et al. and Abe et al. in 2014 and 2015. By driving diode-switches of CWVM by using high speed rectangular pulses, these voltage multipliers can provide an output voltage at high speed, where the rectangular pulses are generated by employing high/low side drivers. However, the number of stages of the CWVM is still large, though these CWVMs [14-16] can achieve high response speed.

To achieve high gain with small number of stages, a high voltage multiplier with series-connected bipolar topology is proposed by Eguchi et al. in 2015 [17]. By connecting positive/negative multiplier blocks in series, the CWVM reported in [17] amplifies the input voltage twice. Therefore, the voltage multiplier reported in [17] can achieve high gain with small number of stages. Following this study, Abe et al. suggested a high voltage multiplier using level shift drivers [18,19] to simplify the circuit configuration. By connecting CWVMs via level shift drivers, Abe et al.'s multiplier can generate a high stepped-up voltage without a full-bridge circuit. However, the circuit configuration of the series-connected voltage multiplier is complex, though the number of stages can be reduced. Furthermore, the voltage multiplier using level shift drivers suffers from high voltage stress. For above-mentioned drawbacks of the conventional multipliers [6-19], an inductor-less high voltage multiplier realizing high gain and small circuit size is required to develop an efficient non-thermal food processing system at low cost.

In this paper, a novel high voltage multiplier is proposed for non-thermal food processing utilizing an underwater shockwave. Unlike the conventional voltage multipliers,

the proposed multiplier is designed by connecting a bipolar CWVM with a switched-capacitor (SC) direct ac-ac converter in series. First, an ac input is amplified to double by the inductor-less ac-ac converter. Then, the output of the ac-ac converter is stepped-up again by the bipolar CWVM. By converting the ac input twice, high step-up gain is realized with a small number of stages. In other words, the proposed multiplier can alleviate the threshold voltage drop caused by diode switches. Furthermore, the proposed multiplier can achieve smaller size than existing multipliers, because the proposed multiplier requires no magnetic components. To clarify circuit characteristics, simulation program with integrated circuit emphasis (SPICE) simulations and theoretical analysis are performed concerning the proposed CWVM.

The remainder of this paper is organized as follows. Section 2 gives the circuit configuration of the proposed high voltage multiplier to expose the difference between the proposed circuit topology and conventional topologies. Section 3 clarifies the characteristics of the proposed multiplier by theoretical analysis. Section 4 demonstrates the results of SPICE simulation to confirm validity of circuit design. Finally, Section 5 discusses conclusion and future work of this study.

2. Circuit Configuration.

2.1. **Block diagram.** Figure 1 illustrates the comparison of the block diagrams between the proposed multiplier and conventional multipliers. As Figure 1 shows, the proposed multiplier is composed of a switched-capacitor (SC) ac-ac converter and a bipolar multiplier. The features of the proposed multiplier are as follows. 1) By employing bipolar topology, the proposed multiplier can alleviate the voltage drop caused by the increase of the number of stages. The number of stages for the proposed multiplier is about a half of the conventional multiplier [5,9]. 2) Unlike conventional multipliers [10,12], the proposed multiplier requires no full waveform rectifier (FWR). Therefore, the proposed multiplier using an ac-ac converter can achieve small and simple circuit configuration. 3) By combining the bipolar CWVM and an ac-ac converter, the input voltage V_{AC} is converted twice. Owing to the series-connected structure, the proposed multiplier can achieve high step-up gain.

2.2. **Circuit configuration.** The circuit configuration of the proposed multiplier is drawn in Figure 2. As Figures 1 and 2 show, the proposed multiplier amplifies the input voltage twice. The operation principle of the proposed multiplier is as follows. First, in the SC ac-ac converter, the input voltage V_{AC} (= 100V@50Hz) is charged to C_1 and C_2 by controlling transistor switches, where high-speed two-phase clock pulses, $\Phi 1$ and $\Phi 2$, are used to drive transistor switches. Since C_1 and C_2 are connected in series, the output voltage of SC ac-ac converter, namely, the input voltage of the bipolar CWVM becomes $2V_{AC}$. Then, the ac input voltage is converted again in the bipolar CWVM. The bipolar CWVM offers a positive output V_{po} and a negative output V_{no}. Concretely, in Figure 2, the outputs V_{po} and V_{no} are about $14V_{\max}$ and $-12V_{\max}$, respectively, where $V_{\max}$ denotes the maximum value of V_{AC}. By combining V_{po} and V_{no}, the output voltage stored in the output capacitor C_{out} becomes as follows:

$$V_{out} = 26V_{\max} - 15V_{th}, \tag{1}$$

where V_{th} denotes the threshold voltage of the diode switch. To destroy fruits and vegetables, the step-up gain is set to 26 in the proposed multiplier, because more than 3.5kV must be generated from 100V@50Hz to destroy target foods.

The comparison of output voltages between the proposed multiplier and conventional CWVMs is shown in Table 1, where N $(= 1, 2, \ldots)$ denotes the number of stages of the

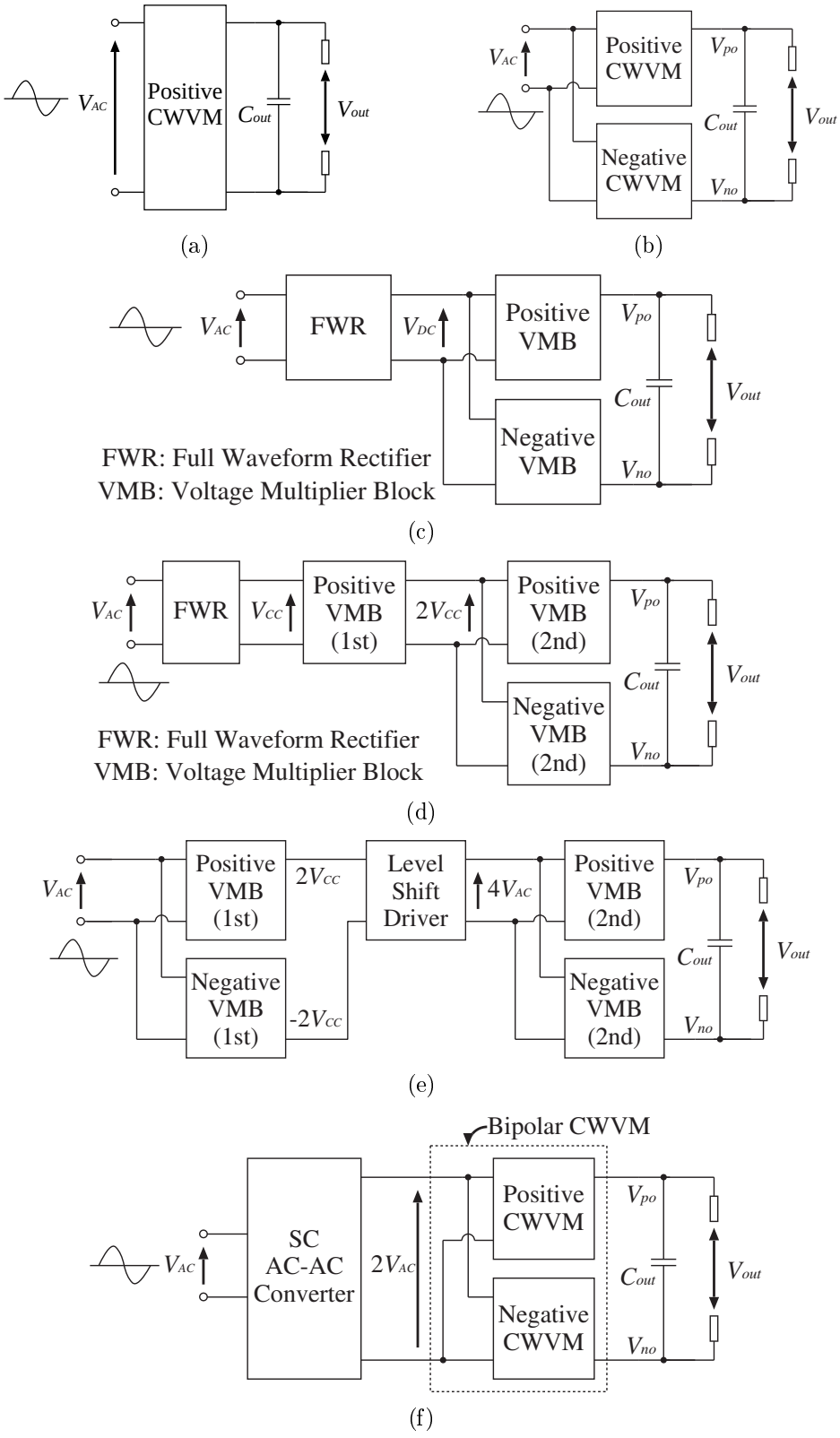

FIGURE 1. Comparison of block diagrams: (a) conventional CWVM [5,9], (b) conventional CWVM [7,8], (c) conventional CWVM [10], (d) conventional CWVM [12], (e) conventional CWVM [13], and (f) the proposed multiplier

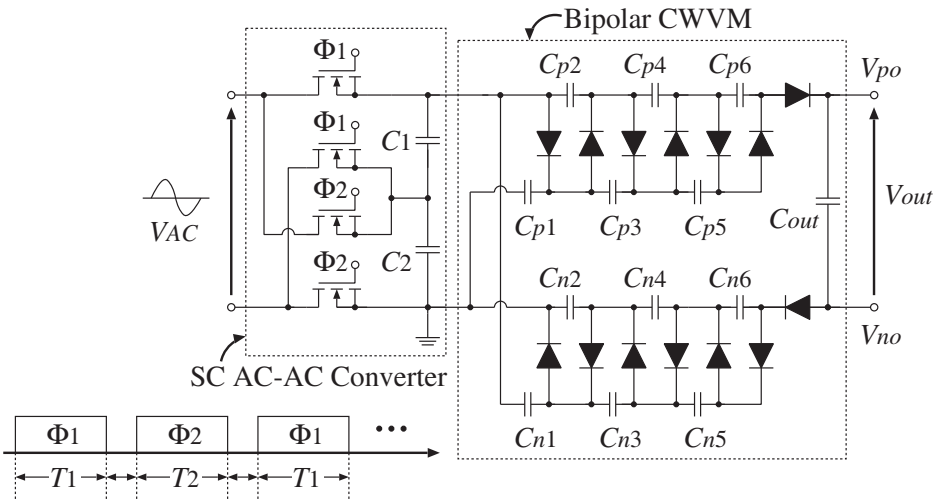

FIGURE 2. Circuit configuration of the proposed multiplier

TABLE 1. Comparison of output voltages

	Output Voltage
Conventional CWVM1 [6,13]	$V_{out} = 2N\,(V_{\max} - V_{th}) = 2NV_{\max} - 2NV_{th}$
Conventional CWVM2 [11,12,14-16]	$V_{out} = 2N\,(V_{\max} - V_{th}) + (2N)\,V_{\max} - (2N+1)\,V_{th}$ $= 4NV_{\max} - (4N+1)\,V_{th}$
Conventional CWVM3 [17]	$V_{out} = 2(2N+1)\,(V_{\max} - V_{th}) + 2(2N)\,(V_{\max} - V_{th}) - V_{th}$ $= (8N+2)\,V_{\max} - (8N+3)V_{th}$
Conventional CWVM4 [18,19]	$V_{out} = 2(4N+1)\,(V_{\max} - V_{th}) - (2N+1)V_{th}$ $+ 2(2N+1)\,(V_{\max} - V_{th}) - (N+1)V_{th}$ $= (12N+4)V_{\max} - (15N+6)V_{th}$
Proposed multiplier	$V_{out} = (2N+1)\,(2V_{\max} - V_{th}) + 2N\,(2V_{\max} - V_{th}) - 2V_{th}$ $= (8N+2)V_{\max} - (4N+3)V_{th}$

VMB. As Table 1 shows, the step-up gain of the proposed multiplier is higher than that of the conventional CWVM1, 2, and 3. Concretely, the proposed multiplier can generate more than 3.5kV when $V_{AC} = 100$V@50Hz and $N = 3$. Of course, the gain of the conventional CWVM4 is higher than that of the proposed multiplier. However, as we described in Section 1, the conventional CWVM4 [18,19] suffers from high voltage stress. Furthermore, the threshold voltage drop caused by diode switches is very large.

3. **Theoretical Analysis.** In the case of the 26× step-up gain, the equivalent model of the proposed multiplier is derived theoretically in order to clarify circuit characteristics. In the theoretical analysis, the four-terminal equivalent circuit reported in [20,21] is used as the equivalent model, where the following conditions are assumed: 1) AC input is a staircase ac waveform, 2) parasitic elements are negligibly small, and 3) time constant is much larger than the period of clock pulses. Figure 3 illustrates the four-terminal equivalent circuit of the proposed multiplier, where m_1, m_2 and m_3 denote the ratio of ideal transformers and R_{SC1} and R_{SC2} are internal resistances called the SC resistance. By using instantaneous equivalent circuits, the parameters of the four-terminal equivalent circuit [20,21], m_1, m_2, m_3, R_{SC1} and R_{SC2}, are derived.

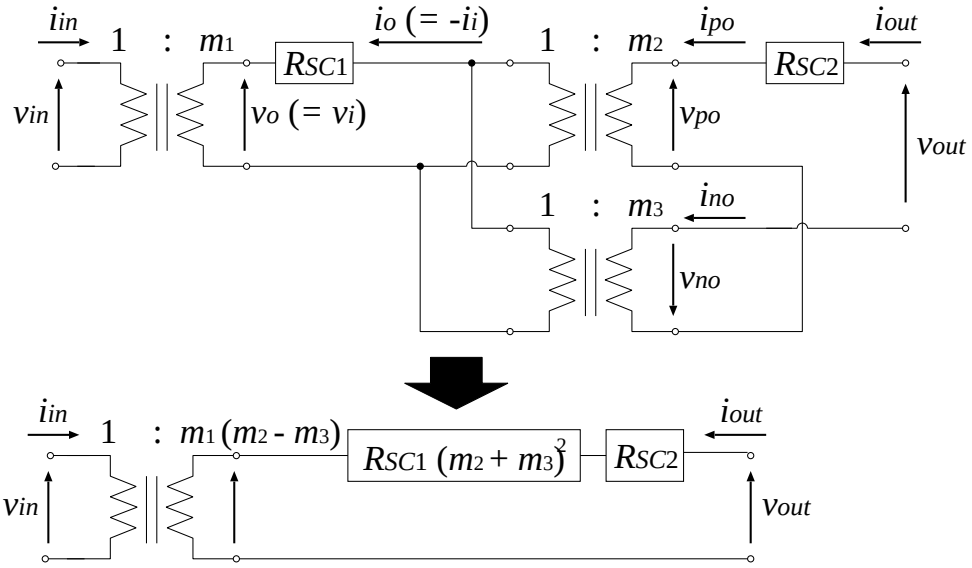

FIGURE 3. Four-terminal equivalent model for the proposed multiplier

Figure 4 illustrates the instantaneous equivalent circuits of the proposed multiplier in steady state. In Figure 4, R_{on} denotes the on-resistance of the transistor switch, R_d denotes the on-resistance of the diode, and V_{th} is the threshold voltage of the diode. In the steady state, the differential value of the electric charge in C_j, C_{pk} and C_{nk} ($(j = 1, 2)$ and $(k = 1, \ldots, 6)$) satisfies

$$\Delta q^j_{T'_1} + \Delta q^j_{T'_2} = 0,\ \Delta q^{pk}_{T_1} + \Delta q^{pk}_{T_2} = 0 \text{ and } \Delta q^{nk}_{T_1} + \Delta q^{nk}_{T_2} = 0, \tag{2}$$

where $\Delta q^j_{T'_i}$ $(i = 1, 2)$ denotes the electric charges of the j-th capacitor in State-T'_i, and $\Delta q^{pk}_{T_i}$ and $\Delta q^{nk}_{T_i}$ denote the electric charges of the k-th capacitor in State-T_i. In (2), the interval of clock pulses satisfies the following conditions:

$$T' = T'_1 + T'_2,\ T'_1 = T'_2 = \frac{T'}{2},\ T = T_1 + T_2, \text{ and } T_1 = T_2 = \frac{T}{2}, \tag{3}$$

where T' and T are the period of clock pulses for the ac-ac converter block and the bipolar CWVM block, respectively, and T'_i and T_i are the pulse width of Φ'_i and Φ_i, respectively.

First, the circuit parameters m_1 and R_{SC1} of the ac-ac converter block are derived. While the state is T'_1 and the ac input is positive, we have the differential values of electric charges in the input and output terminal, $\Delta q_{T'_1, v_{in}}$ and $\Delta q_{T'_1, v_o}$, as follows:

$$\Delta q_{T'_1, v_{in}} = \Delta q^1_{T'_1} - \Delta q^2_{T'_1} \text{ and } \Delta q_{T'_1, v_o} = \Delta q^1_{T'_1} - \Delta q_{T'_1, v_{in}}. \tag{4}$$

While the state is T'_2 and the ac input is positive, the differential values of electric charges in the input and output terminal, $\Delta q_{T'_2, v_{in}}$ and $\Delta q_{T'_2, v_o}$, are given as

$$\Delta q_{T'_2, v_{in}} = \Delta q^2_{T'_2} - \Delta q^1_{T'_2} \text{ and } \Delta q_{T'_2, v_o} = \Delta q^1_{T'_2}. \tag{5}$$

On the other hand, while the state is T'_1 and the ac input is negative, we have the differential values of electric charges, $\Delta q_{T'_1, v_{in}}$ and $\Delta q_{T'_1, v_o}$, as follows:

$$\Delta q_{T'_1, v_{in}} = \Delta q^2_{T'_1} - \Delta q^1_{T'_1} \text{ and } \Delta q_{T'_1, v_o} = -\Delta q^1_{T'_1} - \Delta q_{T'_1, v_{in}}. \tag{6}$$

While the state is T'_2 and the ac input is negative, $\Delta q_{T'_2, v_{in}}$ and $\Delta q_{T'_2, v_o}$ are given as

$$\Delta q_{T'_2, v_{in}} = \Delta q^1_{T'_2} - \Delta q^2_{T'_2} \text{ and } \Delta q_{T'_2, v_o} = -\Delta q^1_{T'_2}. \tag{7}$$

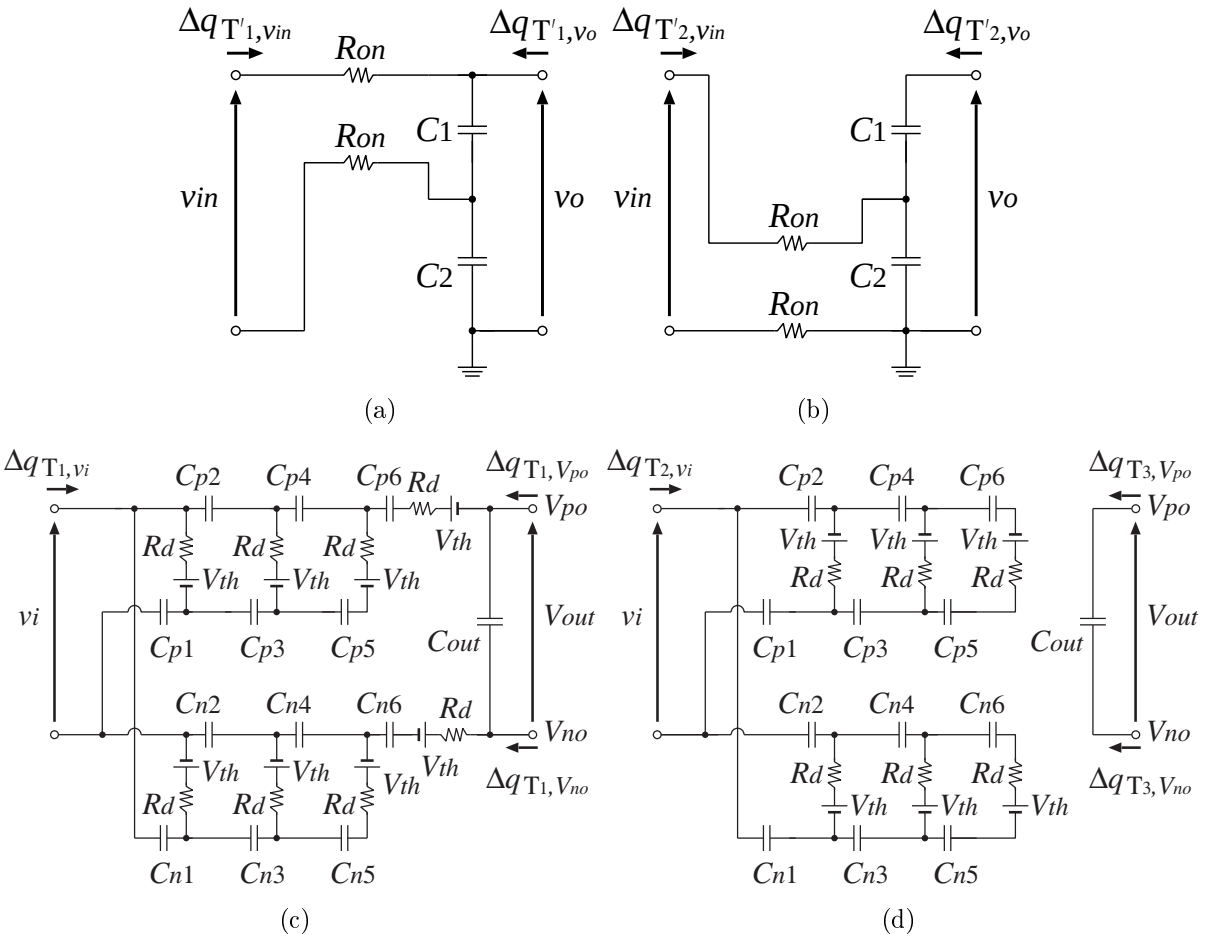

FIGURE 4. Instantaneous equivalent circuits of the proposed multiplier: (a) ac-ac converter block during State-T_1', (b) ac-ac converter block during State-T_2', (c) bipolar CWVM block during State-T_1, and (d) bipolar CWVM block during State-T_2

Here, using the Kirchhoff's current laws, the input and output currents are expressed as

$$i_{in} = \frac{\Delta q_{v_{in}}}{T} = \frac{\Delta q_{T_1',v_{in}} + \Delta q_{T_2',v_{in}}}{T} \text{ and } i_o = \frac{\Delta q_{v_o}}{T} = \frac{\Delta q_{T_1',v_o} + \Delta q_{T_2',v_o}}{T}, \tag{8}$$

because the overall change of the input and output currents is zero in the steady state. In (8), $\Delta q_{v_{in}}$ and Δq_{v_o} are electric charges in v_{in} and v_o, respectively. Substituting (2)-(7) into (8), we have the relation between the input current and the output current as follows:

$$i_{in} = -2i_o. \tag{9}$$

Therefore, the conversion ratio in Figure 3 can be obtained as $m_1 = 2$.

Next, in order to derive the SC resistance R_{SC1} of the ac-ac converter block, the consumed energy in one period is discussed. In spite of the polarity of an ac input, the consumed energy W_T^1 of the ac-ac converter block can be expressed as

$$W_{T'}^1 = W_{T_1'}^1 + W_{T_2'}^1, \tag{10}$$

where

$$W_{T_1'}^1 = \frac{\left(\Delta q_{T_1',v_{in}}\right)^2}{T_1'} \times 2R_{on} \text{ and } W_{T_2'}^1 = \frac{\left(\Delta q_{T_2',v_{in}}\right)^2}{T_2'} \times 2R_{on}. \tag{11}$$

In (10), dielectric loss is not considered to simplify the theoretical analysis. Using (2)-(7), the consumed energy (10) can be rewritten as

$$W_{T'}^{1} = \frac{8R_{on}\left(\Delta q_{v_o}\right)^2}{T'}. \tag{12}$$

Here, the consumed energy W_T of the SC ac-ac converter in Figure 3 is defined as

$$W_T = R_{SC1}\frac{\left(\Delta q_{v_o}\right)^2}{T'}, \tag{13}$$

because energy is consumed by R_{SC1}. Therefore, from (12) and (13), the SC resistance R_{SC1} in the SC ac-ac converter can be obtained as $R_{SC1} = 8R_{on}$.

Next, the circuit parameters of the bipolar CWVM block are analyzed. During State-T_1, the differential values of electric charges in the input and output terminals, $\Delta q_{T_1,v_i}$, $\Delta q_{T_1,v_{po}}$ and $\Delta q_{T_1,v_{no}}$, are given as

$$\Delta q_{T_1,v_i} = \Delta q_{T_1}^{p1} - \Delta q_{T_1}^{p2} - \Delta q_{T_1}^{p3} + \Delta q_{T_1}^{n1},\ \Delta q_{T_1,v_{po}} = \Delta q_{T_1}^{p6} \text{ and } \Delta q_{T_1,v_{no}} = \Delta - q_{T_1}^{n6}, \tag{14}$$

where the following conditions are satisfied:

$$\begin{aligned} &\Delta q_{T_1}^{p6} = \Delta q_{T_1}^{p4} + \Delta q_{T_1}^{p5},\ \Delta q_{T_1}^{p4} = \Delta q_{T_1}^{p2} + \Delta q_{T_1}^{p3} - \Delta q_{T_1}^{p5}, \\ &\Delta q_{T_1}^{n6} = \Delta q_{T_1}^{n4} + \Delta q_{T_1}^{n5} \text{ and } \Delta q_{T_1}^{n4} = \Delta q_{T_1}^{n2} + \Delta q_{T_1}^{n3} - \Delta q_{T_1}^{n5}. \end{aligned} \tag{15}$$

During State-T_2, the differential values of electric charges in the input and output terminals, $\Delta q_{T_2,v_i}$, $\Delta q_{T_2,v_{po}}$ and $\Delta q_{T_2,v_{no}}$, are given as

$$\Delta q_{T_2,v_i} = \Delta q_{T_2}^{p2} - \Delta q_{T_2}^{n1}, \quad \Delta q_{T_1,v_{po}} = 0 \text{ and } \Delta q_{T_1,v_{no}} = 0, \tag{16}$$

where the following conditions are satisfied:

$$\begin{aligned} &\Delta q_{T_2}^{p6} = \Delta q_{T_2}^{p3} + \Delta q_{T_2}^{p4} - \Delta q_{T_2}^{p5},\ \Delta q_{T_2}^{p4} = \Delta q_{T_2}^{p1} + \Delta q_{T_2}^{p2} - \Delta q_{T_2}^{p3}, \\ &\Delta q_{T_2}^{n6} = \Delta q_{T_2}^{n3} + \Delta q_{T_2}^{n4} - \Delta q_{T_2}^{n5} \text{ and } \Delta q_{T_2}^{n4} = \Delta q_{T_2}^{n1} + \Delta q_{T_2}^{n2} - \Delta q_{T_2}^{n3}. \end{aligned} \tag{17}$$

As in the case of (8), the input and output currents are defined as

$$\begin{aligned} &i_i = \frac{\Delta q_{v_i}}{T} = \frac{\Delta q_{T_1,v_i} + \Delta q_{T_2,v_i}}{T},\ i_{po} = \frac{\Delta q_{v_{po}}}{T} = \frac{\Delta q_{T_1,v_{po}} + \Delta q_{T_2,v_{po}}}{T} \\ &\text{and } i_{no} = \frac{\Delta q_{v_{no}}}{T} = \frac{\Delta q_{T_1,v_{no}} + \Delta q_{T_2,v_{no}}}{T}, \end{aligned} \tag{18}$$

where Δq_{v_i}, $\Delta q_{v_{po}}$ and $\Delta q_{v_{no}}$ are electric charges in v_{in}, v_{po} and v_{no}, respectively. Substituting (2), (14)-(17) into (18), we have the relation between the input current and the output currents as follows:

$$i_i = -7i_{po} + 6i_{no}. \tag{19}$$

Therefore, the conversion ratios in Figure 3 can be obtained as $m_2 = 7$ and $m_3 = 6$.

Next, we discuss the consumed energy W_T^2 in one period to derive the SC resistance R_{SC2} of the bipolar CWVM block. As is the case in (10), the consumed energy W_T^2 of the bipolar CWVM block can be expressed as

$$W_T^2 = W_{T_1}^2 + W_{T_2}^2, \tag{20}$$

where

$$W_{T_1}^2 = \frac{\left(\Delta q_{T_1}^{p1} - \Delta q_{T_1}^{p3}\right)^2}{T_1} \times r_d + \frac{\left(\Delta q_{T_1}^{p3} - \Delta q_{T_1}^{p5}\right)^2}{T_1} \times r_d + \frac{\left(\Delta q_{T_1}^{p5}\right)^2}{T_1} \times r_d + \frac{\left(\Delta q_{T_1}^{p6}\right)^2}{T_1} \times r_d + \frac{\left(\Delta q_{T_1}^{n1} - \Delta q_{T_1}^{n3}\right)^2}{T_1} \times r_d + \frac{\left(\Delta q_{T_1}^{n3} - \Delta q_{T_1}^{n5}\right)^2}{T_1} \times r_d + \frac{\left(\Delta q_{T_1}^{n5}\right)^2}{T_1} \times r_d + \frac{\left(\Delta q_{T_1}^{n6}\right)^2}{T_1} \times r_d \tag{21}$$

$$\text{and } W_{T_2}^2 = \frac{\left(\Delta q_{T_2}^{p1} - \Delta q_{T_2}^{p3}\right)^2}{T_2} \times r_d + \frac{\left(\Delta q_{T_2}^{p3} - \Delta q_{T_2}^{p5}\right)^2}{T_2} \times r_d + \frac{\left(\Delta q_{T_2}^{p5}\right)^2}{T_2} \times r_d + \frac{\left(\Delta q_{T_2}^{n1} - \Delta q_{T_2}^{n3}\right)^2}{T_2} \times r_d + \frac{\left(\Delta q_{T_2}^{n3} - \Delta q_{T_2}^{n5}\right)^2}{T_2} \times r_d + \frac{\left(\Delta q_{T_2}^{n5}\right)^2}{T_2} \times r_d.$$

Using (2), (14)-(17), the consumed energy (20) can be rewritten as

$$W_T^2 = \frac{14 r_d \left(\Delta q_{v_{po}}\right)^2}{T} + \frac{14 r_d \left(\Delta q_{v_{no}}\right)^2}{T} = \frac{28 r_d \left(\Delta q_{v_{out}}\right)^2}{T}, \tag{22}$$

where

$$\Delta q_{v_{po}} = -\Delta q_{v_{no}} = \Delta q_{v_{out}}. \tag{23}$$

Therefore, from (13) and (22), the SC resistance R_{SC2} in Figure 3 can be obtained as $R_{SC2} = 28 r_d$. By combining m_1, m_2, m_3, R_{SC1} and R_{SC2}, the equivalent circuit is obtained as

$$\begin{bmatrix} v_{\max} - \left(\frac{15}{26}\right) V_{th} \\ i_{in} \end{bmatrix} = \begin{bmatrix} 1/26 & 0 \\ 0 & 26 \end{bmatrix} \begin{bmatrix} 1 & 1352 R_{on} + 28 r_d \\ 0 & 1 \end{bmatrix} \begin{bmatrix} v_{out} \\ -i_{out} \end{bmatrix}, \tag{24}$$

because the four-terminal equivalent circuit of Figure 3 can be expressed by the K-matrix. From (24), the output voltage of the proposed multiplier is derived as

$$v_{out} = \left\{ \frac{R_L}{(1352 R_{on} + 28 r_d) + R_L} \right\} \left(26 v_{\max} - 15 V_{th}\right). \tag{25}$$

4. **Simulation.** The characteristics of the proposed multiplier are demonstrated by SPICE simulations. In SPICE simulations, the target output voltage was set to 3.5kV, because the 3.5kV output has been used to generate an underwater shockwave in previous studies. Figure 5 demonstrates the simulated output voltages of the proposed multiplier, where the SPICE simulation was performed under conditions that $V_{ac} = 100$V@50Hz, $T = 100\mu$s, $T_1' = T_2' = 50\mu$s, $C_1 = C_2 = 10\mu$F, and $C_{p1} = \ldots = C_{p6} = C_{n1} = \ldots = C_{n6} = C_{out} = 33\mu$F. In other words, the transistor switches of the SC ac-ac converter were driven by the clock pulses at 10kHz. Therefore, a general discrete component can be available as the transistor switch in the proposed multiplier. As Figure 5 shows, the proposed multiplier can generate more than 3.5kV within 2.65 seconds. On the other hand, Figure 6 demonstrates the output voltage of the traditional CWVM reported in [6], where the SPICE simulation was performed under conditions that the step-up gain is 26, the input voltage is 100V@50Hz, and all the capacitances are 33μF. As Figure 6 shows, the traditional CWVM takes about 79.5 seconds to generate 3.5kV. From these results, the proposed multiplier is much faster than the traditional CWVM reported in [6]. Concretely, the startup time of the proposed multiplier is less than 1/30 of that of the traditional CWVM reported in [6].

Figure 7 shows the result of the Monte Carlo analysis for the proposed multiplier, where capacitors have 20% tolerance with Gaussian distribution. In Figure 7, the mean value

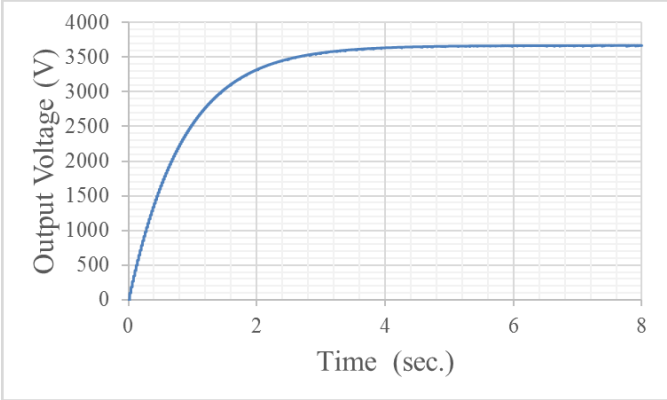

FIGURE 5. Simulated output voltage of the proposed multiplier

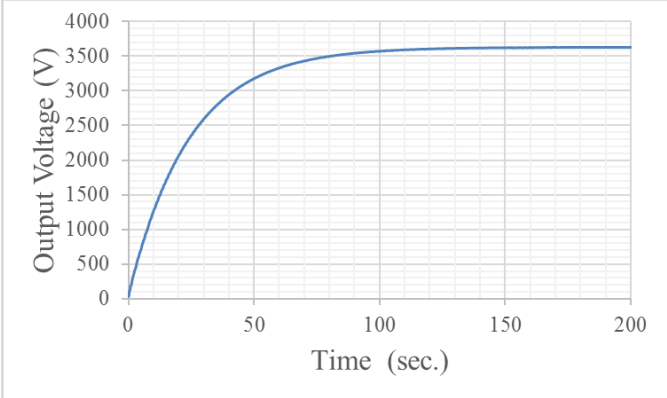

FIGURE 6. Simulated output voltage of the traditional CWVM [6]

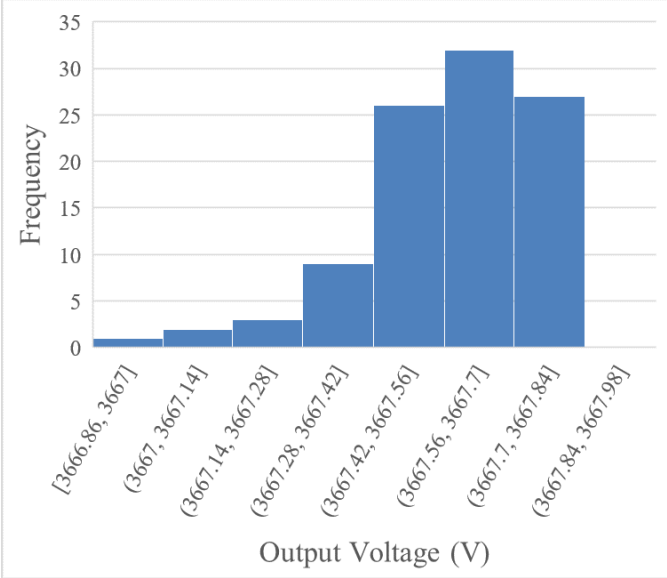

FIGURE 7. Result of the Monte Carlo simulation for the proposed multiplier

is 3.67kV and the standard deviation is 0.18V. On the other hand, Figure 8 shows the result of the Monte Carlo analysis for the traditional CWVM reported in [6]. In Figure 8, the mean value is 3.63kV and the standard deviation is 1.01V. As the results Figures

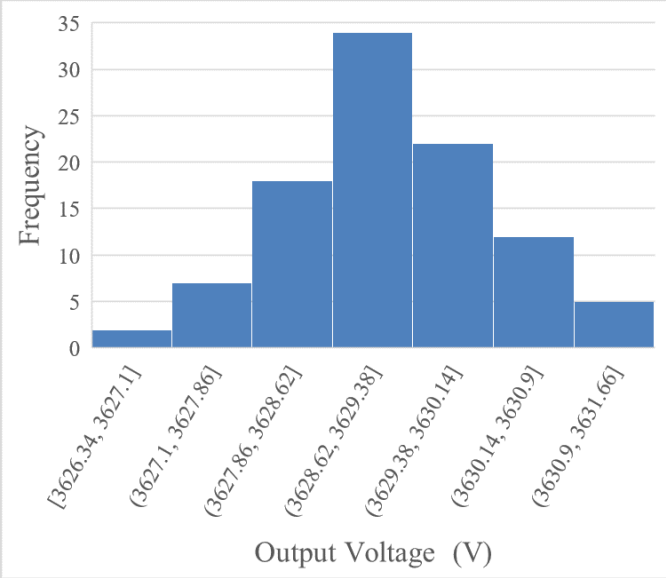

FIGURE 8. Result of the Monte Carlo simulation for the traditional CWVM [6]

TABLE 2. Comparison of the number of circuit components

	Number of diodes	Number of capacitors	Number of switches
Conventional CWVM [6]	26	26	0
Conventional CWVM [14]	62	43	4
Conventional CWVM [17]	34	29	8
Conventional CWVM [18,19]	24	18	4
Proposed multiplier	14	14	4

TABLE 3. Summary of simulation results

	Value
Number of circuit components	14 diodes, 14 capacitors, and 4 transistor switches
Output voltage	3.67kV (V_{ac} = 100V@50Hz)
Standard deviation of V_{out}	0.18V (20% capacitor tolerance)
Rise time	2.65 seconds (Gain 26×)

7 and 8 show, the proposed multiplier as well as the traditional CWVM is robust to the fluctuation of capacitors.

Table 2 shows the comparison of the number of circuit components between the proposed CWVM and conventional CWVMs reported in [6,14,17-19]. In Table 2, the conventional CWVMs using transformers are omitted. As Table 2 shows, the proposed multiplier can be fabricated by 14 diodes, 14 capacitors, and 4 transistor switches. The number of circuit components for the proposed multiplier is smaller than that for the conventional CWVMs [6,14,17-19] though the conventional CWVMs reported in [14,17-19] are faster than the proposed CWVM. Concretely, the proposed multiplier can reduce more than 38% of circuit components from the traditional CWVM reported in [6]. The result of SPICE simulations is summarized in Table 3.

5. **Conclusions.** For non-thermal food processing utilizing an underwater shockwave, a novel high voltage multiplier has been proposed in this paper. By connecting an SC ac-ac converter and a bipolar CWVM in series, the proposed multiplier amplifies the input voltage twice with small number of circuit components. Furthermore, the proposed multiplier can be realized without a full waveform rectifier as well as a magnetic component.

Concerning the proposed multiplier with 14 diodes, 14 capacitors, and 4 transistor switches, the characteristic evaluation was performed through theoretical analysis and SPICE simulations. By converting the input voltage 100V@50Hz, more than 3.5kV output was generated by the proposed voltage multiplier. The proposed multiplier was robust to the fluctuation of capacitors. Concretely, the standard deviation of the output voltage was less than 0.18V when capacitors have 20% tolerance with Gaussian distribution. When the gain is 26, the number of circuit components for the proposed voltage multiplier was smaller than that for the inductor-less conventional CWVMs. Concretely, the proposed multiplier reduced more than 38% of circuit components from the traditional CWVM. Therefore, simple circuit configuration can be provided by the proposed voltage multiplier. Furthermore, the proposed voltage multiplier showed higher response speed than the traditional CWVM. Concretely, the startup time of the proposed multiplier was less than 2.65 seconds. As a result of comparison, the startup time of the proposed multiplier was 1/30 of that of the traditional CWVM.

Future work is focused towards the characteristic evaluation of the proposed multiplier through experiments.

Acknowledgment. This research was financially supported by the Urakami Foundation for Food and Food Culture Promotion. The authors also gratefully acknowledge the helpful comments and suggestions of the reviewers, which have improved the presentation.

REFERENCES

[1] M. Stoica, L. Mihalcea, D. Bprda and P. Alexe, Non-thermal novel food processing technologies. An overview, *Journal of Agroalimentary Processes and Technologies*, vol.19, no.2, pp.212-217, 2013.

[2] C. H. Zhang, T. Namihira, T. Kiyan, K. Nakashima, S. Katsuki, H. Akiyama, H. Ito and Y. Imaizumi, Investigation of shockwave produced by large volume pulsed discharge under water, *IEEE Pulsed Power Conf.*, pp.1377-1380, 2005.

[3] Y. Miyafuji, K. Shimojima, S. Tanaka, K. Naha, T. Aka, H. Maehara and S. Itoh, Development of the pressure vessel for manufacturing the rice-powder using the underwater shock wave, *Proc. of the ASME 2011 Pressure Vessels and Piping Conf.*, pp.53-56, 2011.

[4] K. Naha, K. Shimojima, Y. Miyafuji and S. Itoh, Design and development of pressure vessel for improvement of manufacturing rice-powder efficiency using underwater shock wave, *Proc. of the ASME 2012 Pressure Vessels and Piping Conf.*, pp.15-19, 2012.

[5] S. Shinzato, Y. Higa, T. Tamaki, H. Iyama and S. Itoh, Computational simulation of underwater shock wave propagation using smoothed particle hydrodynamics, *Materials Science Forum*, vol.767, pp.86-91, 2013.

[6] A. Lamantia, P. Maranesi and L. Radrizzani, The dynamics of the Cockcroft-Walton voltage multiplier, *Proc. of the IEEE Power Electronics Specialists Conf.*, pp.485-490, 1990.

[7] J. Wang and P. Luerkens, Complete model of parasitic capacitances in a cascade voltage multiplier in the high voltage generator, *Proc. of the IEEE ECCE Asia Downunder*, pp.18-24, 2013.

[8] P. S. Patel and D. B. Dave, Design, analysis & implementation of negative high voltage DC power supply using voltage multiplier circuits, *International Journal of Engineering Trends and Technology*, vol.4, no.4, pp.702-706, 2013.

[9] C. H. Young and M. H. Chen, A novel single-phase ac to high voltage dc converter based on Cockcroft-Walton cascade rectifier, *Proc. of the PEDS*, pp.822-826, 2009.

[10] C. H. Young, C. C. Ko, M. H. Chen and C. C. Wu, A Cockcroft-Walton voltage multiplier with PFC using ZC-ZVT auxiliary circuit, *Proc. of the IECON*, pp.1001-1005, 2011.

[11] S. Iqbal and R. Besar, A bipolar Cockcroft-Walton voltage multiplier for gas lasers, *American Journal of Applied Sciences*, vol.4, no.10, pp.795-801, 2007.

[12] K. Eguchi, I. Oota, S. Terada and H. Zhu, 2x/3x step-up switched-capacitor (SC) AC-DC converters for RFID tags, *International Journal of Intelligent Engineering and Systems*, vol.4, no.1, pp.1-9, 2011.

[13] S. Iqbal, A hybrid symmetrical voltage multiplier, *IEEE Trans. Power Electronics*, vol.29, no.1, pp.6-12, 2014.

[14] K. Eguchi, S. Pongswatd, S. Terada and I. Oota, Parallel-connected high voltage multiplier with symmetrical structure, *Applied Mechanics and Materials*, vol.619, pp.173-177, 2014.

[15] K. Eguchi, I. Oota, S. Terada and K. Fujimoto, Design of an inductor-less bipolar voltage multiplier for high-voltage low-current applications, *ICIC Express Letters, Part B: Applications*, vol.6, no.1, pp.1-6, 2015.

[16] K. Abe, H. Sasaki, I. Oota and K. Eguchi, Improvement of an output voltage efficiency of a high voltage generator for non-thermal food processing systems, *ICIC Express Letters*, vol.9, no.11, pp.3087-3092, 2015.

[17] K. Eguchi, K. Abe, H. Fujisawa and I. Oota, Design of a high voltage multiplier with series-connected bipolar topology, *Proc. of the 3rd Intl. Conf. on Advances in Applied Science and Environmental Technology*, pp.113-117, 2015.

[18] K. Abe, I. Oota, W. Do and K. Eguchi, Synthesis of a high step-up bipolar voltage multiplier using level shift drivers, *Proc. of the 6th International Workshop on Computer Science and Engineering*, pp.305-309, 2016.

[19] K. Abe, R. Ogata, K. Eguchi, K. Smerpitak and S. Pongswatd, Study on non-thermal food processing utilizing an underwater shockwave, *Indian Journal of Science and Technology*, vol.10, no.4, pp.1-5, 2017.

[20] K. Eguchi, I. Oota, S. Terada and H. Zhu, Synthesis and analysis of a switched-capacitor-based battery equalizer using level-shift circuits, *International Journal of Intelligent Engineering and Systems*, vol.5, no.4, pp.1-9, 2012.

[21] K. Eguchi, K. Fujimoto and H. Sasaki, A hybrid input charge-pump using micropower thermoelectric generators, *IEEJ Trans. Electrical and Electronic Engineering*, vol.7, no.4, pp.415-422, 2012.